MNRAS **000**, 1–7 (2017) Preprint 1 November 2017 Compiled using MNRAS LATEX style file v3.0

Influence of the reduced light speed approximation on reionization fronts speeds in cosmological RHD simulations

Nicolas Deparis[1]★, Dominique Aubert[1], Pierre Ocvirk[1]
[1] *Observatoire Astronomique de Strasbourg, CNRS UMR 7550, Universite de Strasbourg, Strasbourg,France*

Accepted XXX. Received YYY; in original form ZZZ

ABSTRACT
We run a set of radiative hydrodynamic cosmological simulations of reionization to explore the link between the propagation of ionization and the reduced speed of light approximation. We introduce a method to compute the ionization fronts speeds based on the reionization redshift map a posteriori. We found that for a reduced speed of light greater than $\tilde{c} = 0.05$, the front speed is limited only at the end of the reionization. In the case of a lower reduced speed of light, the RSLA leads to limited front speeds during the whole reionization process.

Key words: cosmology: dark ages, reionization, first stars - methods: numerical

1 INTRODUCTION

A central process to consider when simulating the Epoch of Reionization (EoR) is the light propagation through the Universe. As light is several order faster than hydrodynamical processes generally considered in cosmological simulations, introducing radiative transfer (RT) can be computationally challenging.

There are two main families of RT codes in EoR simulations:

- Ray tracing/Monte Carlo methods consider light as group of photons (eg. CRASH Maselli et al. (2003), C^2-RAY Mellema et al. (2006)). Each source launches a given number of photons along straight lines.
- Moment based methods consider light as a fluid (eg. OTVET Gnedin & Abel (2001a), ATON Aubert & Teyssier (2008)). Each source acts as a fountain where light flows out according to conservation equations on radiative quantities.

Each family has its own pros and cons. The main drawback of the ray-tracing techniques is the computational cost which is directly linked to the number of sources and can be quite prohibitive in cosmological simulations. At the opposite, moment-based methods can be more inaccurate on certain physical effects (e.g. the shadowing effect by dense clump or the collisionless nature of light) but is independent of the number of sources : for this reason it gained some popularity in recent implementations of cosmological radiative transfer. Another key difference is the way they treat the *speed of light* : ray-tracing techniques usually assume an infinite speed of light and photons packets/groups/density are depleted from site to site along rays without including any kind of delay. This assumption is reasonable as light velocities are much larger than for any other processes.

Meanwhile, moment-based methods have to assume a finite speed-of-light as they model the actual propagation of radiation density. This is not without consequences, especially since this fluid description is often handled through an explicit approach (even though implicit solvers do exist see e.g. González et al. (2007)). The main constraint for explicit moment-based solvers is due to the Courant-Friedrichs-Lewy (CFL) condition. It imposes that the higher the velocity of a process is, the higher the temporal resolution has to be to accurately simulate its propagation. The time step Δt is computed using:

$$\Delta t = C_{CFL} \cdot \frac{\Delta x}{v}, \quad (1)$$

where $C_{CFL} < 1$, Δx is the spatial resolution and v is the speed of the considered process. As light has the highest known velocity, it requires a small Δt and a large amount of timesteps to follow its propagation on a given period.

Several methodologies have emerged to reduce this cost. The first one consists in taking profit of the recent hardware evolution: for example, using Graphical Processing Units (GPUs) can divide the computational time by almost two orders of magnitude due to their highly parallel capability. The second method is the one we are looking at in this study, the reduced speed of light approximation (RSLA) (Gnedin & Abel 2001b; Aubert & Teyssier 2008). The main idea of this technique relies on the fact that the speed of dynamical processes (DM and gas) is several orders of magnitude lower than the physical speed of light. As the light speed is significantly greater than any other one, lowering its value in a simulation should not have a significant impact on the

★ E-mail: nicolas.deparis@astro.unistra.fr

results, while at the same time allowing a comfortable gain on the computational cost.

The RSLA considers that the light evolves at a fraction of its real speed:

$$v = \tilde{c} \cdot c, \tag{2}$$

where c is the physical light speed and $\tilde{c} \leq 1$ is the RSLA factor. If the reionization history stays the same between $\tilde{c} = 1$ and $\tilde{c} = 0.1$, we could gain a factor ten in the computation of radiative processes, which is really appreciable as radiation represents approximately 80% of the computational cost in this kind of simulation when $\tilde{c} = 1$.

In this study, we aim at investigating the validity of this approximation and we explore how reducing the speed of light influences the evolution of ionization fronts during the reionization epoch. First we present a set of RHD simulations with different RSLA and introduce a method to compute the reionization fronts speeds using reionization redshift maps. Then, using different diagnostics (average ionization history, ionization maps, fronts speeds), we quantify the impact of reduced speed of light on the global reionization. We briefly conclude with some implications of our results.

2 METHODOLOGY

Simulations are produced with `EMMA` an AMR cosmological code with fully coupled radiative hydrodynamic (Aubert et al. 2015). The light is considered as a fluid, its propagation is tracked using the moment-based M1 approximation (Levermore 1984; González et al. 2007; Aubert & Teyssier 2008).

We run a set of small simulations at a similar resolution of production runs like eg CODA (Ocvirk et al. 2015) or CROC (Gnedin 2014). We are considering $\left(8h^{-1}\mathrm{cMpc}\right)^3$ volumes, simulated from redshift z=150 to the end of the reionization ($5 < z < 6$). Dark matter is resolved with 256^3 particles with a mass of $3.4 \cdot 10^6 M_\odot$. Hydrodynamics and radiation are simulated on a grid 256^3 resolution elements for a coarsest spatial resolution of 46 ckpc. The grid is refined according to a semi-Lagrangian scheme and the refinement is not allowed if the spatial resolution of the newly formed cells is under 500pc. Our stellar mass resolution is set to be equal to $7.2 \cdot 10^4 M_\odot$. We calibrate our emissivity model using Starburst99, with a population of $10^6 M_\odot$ having a Top-Heavy initial mass function and a Z=0.001 metalicity. To limit the number of unknowns, we do not consider supernovae feedback here.

All simulations are run with the exact same parameters (including star formation) and initial conditions, except for $\tilde{c}$, the ratio between the simulated speed of light over the real light speed. We run a set of six simulations with $\tilde{c} = 1$, $\tilde{c} = 0.3$,$\tilde{c} = 0.1$, $\tilde{c} = 0.05$, $\tilde{c} = 0.02$ and $\tilde{c} = 0.01$.

3 RESULTS

3.1 Cosmic star formation and ionization histories

Fig 1a presents the cosmic star formation histories (SFH) as a function of the RSLA. This measure shows that the RSLA does not change the cosmic SFH. And as ionizing photons are emitted by newly formed stars, the photons budget is not impacted of the RSLA.

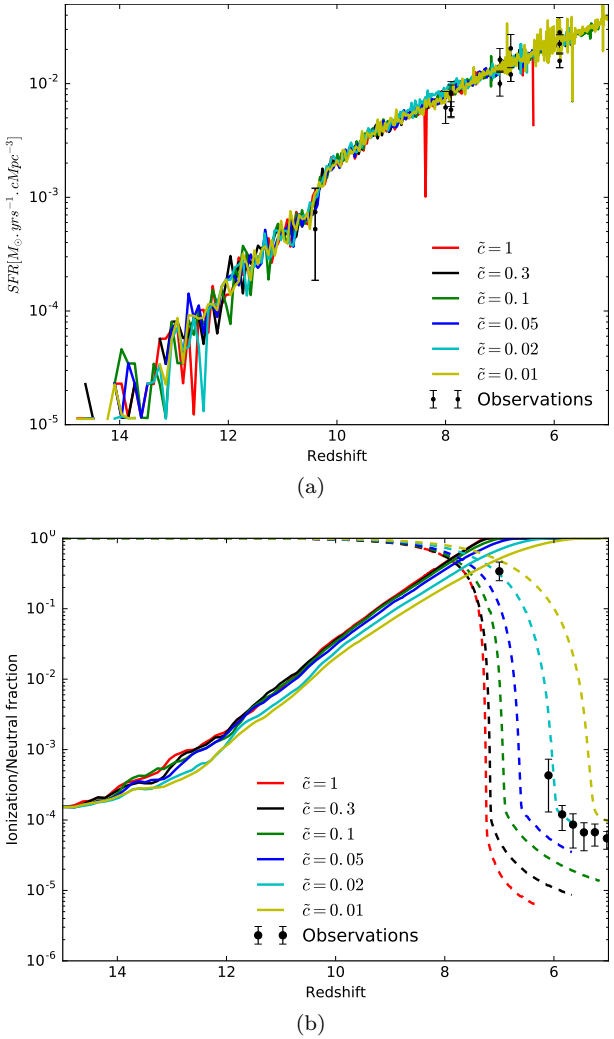

Figure 1. (a) Cosmic star formation histories with observational constraints from Bouwens et al. (2015) ; (b) volume weighted ionization with observational constraints from Fan et al. (2006) (solid lines) and neutral (dashed lines) fraction function of redshift for different reduced speed of light. (c) Reionization redshift function of RSLA.

Fig 1b presents the average volume weighted ionization state as a function of time $X_V(t)$:

$$X_V(t) = \frac{\int x_{(t)} \cdot dV}{\int dV}, \tag{3}$$

with the local ionization fraction :

$$x_{(t)} = \frac{n_{H+}}{n_H} \tag{4}$$

We observe a direct link between the ionization history and the RSLA. The slower the light is, the later the reionization occurs. We define the reionization redshift as the redshift when the volume weighted hydrogen neutral fraction decreases below $X_V = 10^{-4}$. At these times the percolation process of HII regions (also known as *the overlap*) is

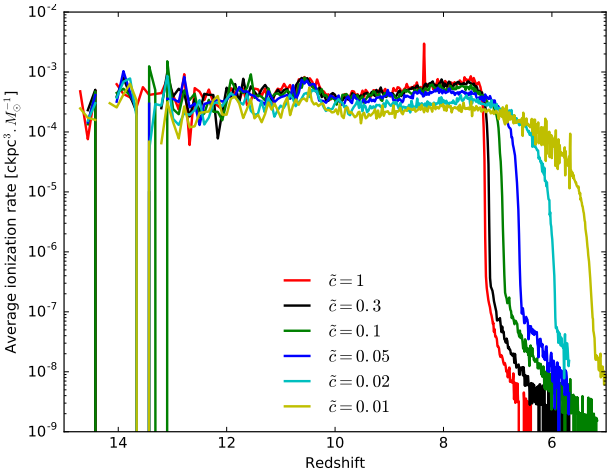

Figure 2. Stellar mass weighted average ionization rate as a function of redshift for different reduce speed of light.

complete. Fig 1c presents obtains reionization redshift as a function of the reduced speed of light. Reionization redshifts converges as $\tilde{c}$ is close to 1, There is a priori no reason for reionization redshift to converge with $\tilde{c} = 0.1$, but this observation may be a point in favour of infinite speed of light techniques: the slope flattening indicates that any $\tilde{c} > 0.1$ lead to the same instant of reionization, a condition trivially satisfied with $c = \infty$. Conversely, reionization redshifts rapidly decline with $\tilde{c}$. For instance, $\tilde{c} = 0.1$ presents a delay of ≈ 60 Myr and less than 0.5 in redshift but these values are extended to ≈ 425 Myr and almost 2.2 in redshift for the $\tilde{c} = 0.01$ run.

It is plausible that the faster the light is, the sooner the photon could reach the under-dense regions, and then the sooner the reionization can occur. But ionization processes limit photon propagation : if this limit would lead to negligible speeds compared to the speed of light, one would expect the RSLA to have no impact on the reionization history. However this is not what is measured here and fronts speeds have to be non negligible compared to speed of light : we assess this point directly in the next sections.

3.2 Average ionization rate

From the previous section we observe that with the same SFR, the ionization history change with the RSLA, so the capacity of stars to reionize their environment is evolving with the light speed. In this section we quantify this effect by introducing a stellar mass weighted average ionization rate.

First we define de the average ionization rate $\dot{X}_{(t)}$ as the temporal derivative of the ionization history.

$$\dot{X}_{(t)} = \frac{dlX_{(t)}}{dt} = \left[\mathrm{yr}^{-1}\right]. \quad (5)$$

By dividing the average ionization rate $\dot{X}_{(t)}$ by the average star formation rate $\dot{\rho}^*_{(t)}$ in $\left[M_\odot \cdot yr^{-1} \cdot ckpc^{-3}\right]$, we quantify the ability of newly formed stars to ionize their environment :

$$\dot{X}_{(\dot{\rho}^*)} = \frac{\dot{X}_{(t)}}{\dot{\rho}^*_{(t)}}\left[\mathrm{ckpc}^3 \cdot \mathrm{M}_\odot^{-1}\right]. \quad (6)$$

It represents the amount of volume each solar masses of stars, newly formed in the simulation, will reionize. The resulting stellar mass weighted ionization rate computation is presented on Fig. 2 as a function of redshift and RSLA. Each run gets an almost flat ionization rate before redshift z=8. In this phase the ionization rate is governed by the star formation and tends to be independent of the RSLA for runs with $\tilde{c} \geq 0.05$, but is lowered for $\tilde{c} < 0.05$.

During this flat phase, the average ionization rate before z=8 are going from $5.1 \cdot 10^{-4}$ ckpc^3.$M_\odot^{-1}$ for the $\tilde{c} = 1$ run, to $2.4 \cdot 10^{-4}$ ckpc^3.$M_\odot^{-1}$ for the $\tilde{c} = 0.01$ run.

The main difference comes later for redshift $z < 8$, where light reaches under-dense regions and ionized bubbles start to merge. It becomes more difficult for the radiation emitted by newly formed stars to ionize neutral medium as the neutral gas is rarer. This transition happens almost instantaneously with $\tilde{c} = 1$ and is more progressive with smaller light speeds.

3.3 Ionization maps

Ionization redshift maps offer an insteresting tool to analyse the whole reionization process using a single data field. Redshift maps are obtained by keeping in memory, for each cell, the time when its ionization fraction pass a given threshold. The computation is done during simulation runtime to get the highest temporal resolution possible. In this study, the cell reionization time is considered to be the first time when the volume weighted ionization fraction passes through 50%.

Fig. 3 shows three maps of reionization redshifts for three RSLA, and the reionization redshift probability density function (PDF) for all runs. Maps are one coarse cells (46 ckpc) thick slices taken at the same coordinate in the z axis for the three simulations. The slice is chosen to contain the first cell to cross the ionization threshold in the $\tilde{c} = 0.1$ simulation.

We observe a similar global behaviour between runs. The sources are located at the same places independently of the run, which is coherent with the fact that the ionizing feedback does not significantly change global star formation processes in our simulation (Fig 1a). Radiation escapes high density regions in comparable butterfly shapes.

The $\tilde{c} = 0.1$ run is quite similar to the the $\tilde{c} = 1$. Dark green isocontours ($z \approx 6$) are located at the same place and have the same shape. The main difference between these runs appears at low redshift when the light reaches the voids (blue shades). Voids reionize a bit slower at $\tilde{c} = 0.1$ than at $\tilde{c} = 1$ due to the time taken by light to reach them. The behaviour is even more pronounced for $\tilde{c} = 0.01$ where the voids reionization is clearly late compared to the two other panels.

This is particularly clear regarding the redshifts PDF : at high redshifts all PDF are similar, but the difference slowly increases with time, and the cumulative effect leads to a significant delay on the global reionization. This is in accordance with the observations made on the volume weighted

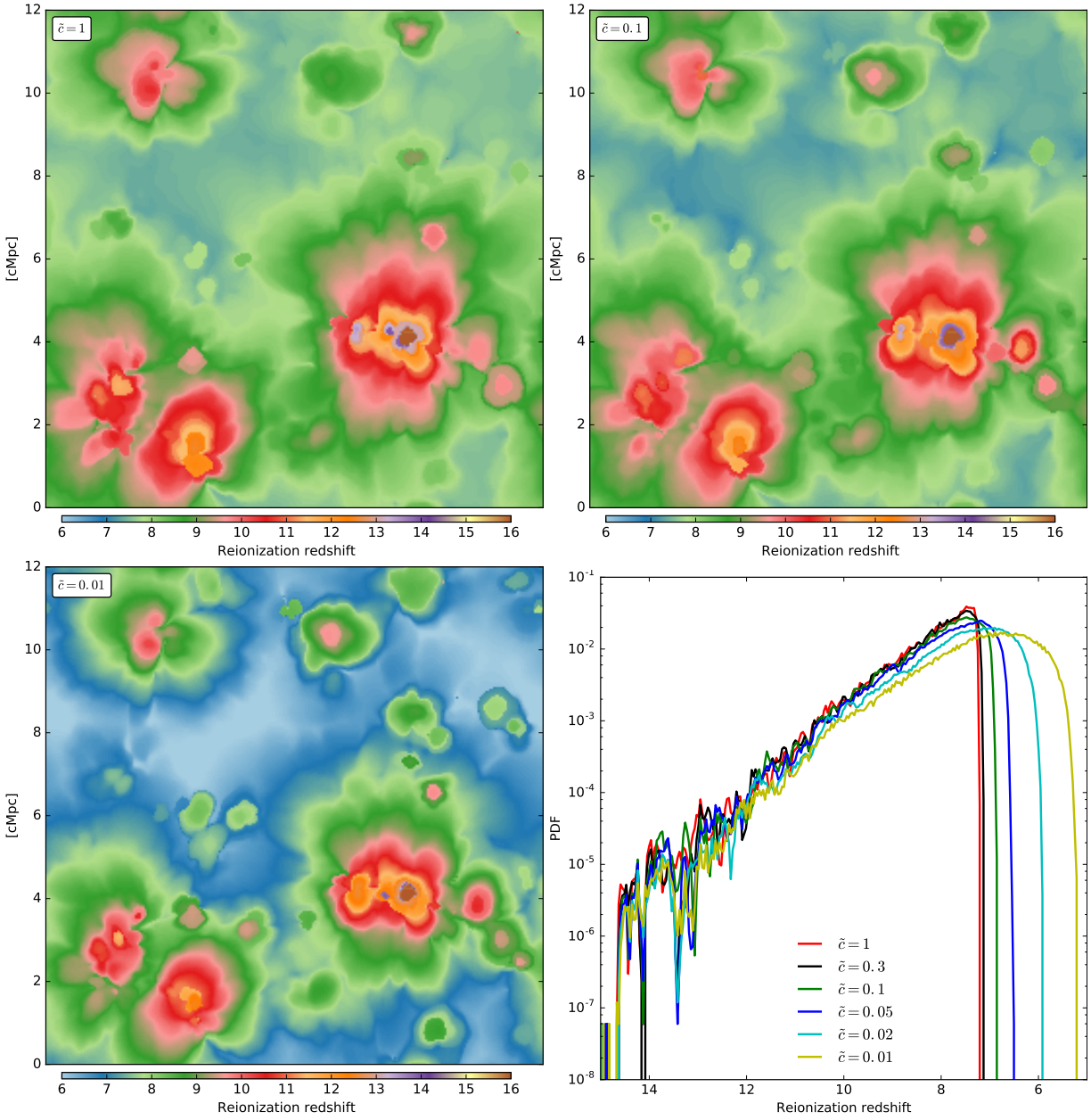

Figure 3. Maps and PDF of reionization redshifts for runs with different reduced speed of light.

ionization history (Fig. 1b), as the voids represent the major part of the volume : runs with faster light reionize faster, due to the ability of light to reach voids sooner.

3.4 Ionization fronts speeds

The reionization maps represent a time at each point of the space. Considering the spatial gradient of this map, we obtain the information of the time needed to reionize each cells.

We use a discrete gradient with the form:

$$\vec{\nabla} t^i_{reio} \approx \frac{t^{i+1} - t^{i-1}}{2a^i \left(x^{i+1} - x^{i-1}\right)}. \quad (7)$$

This gradient represents the time needed to ionize a given distance (eg in [yr.pc^{-1}]), the reverse of this gradient is analogue to a velocity (eg in [pc.yr^{-1}]) :

$$V_{reio} = \frac{1}{\left|\vec{\nabla} t_{reio}\right|}. \quad (8)$$

V_{reio} can be interpreted as an estimator to the speed of the reionization front passing through the cell.

Fig. 4 shows maps of reionization front speed obtained with this method for three runs with different reduced speeds of light. Reionization speed can be greater than the speed of light in the simulation, up to several time. This limiting case occurs when neighbouring cells reionize at the same timestep, their gradient became null and the associated reionization speeds become infinite. This can happen in two cases:

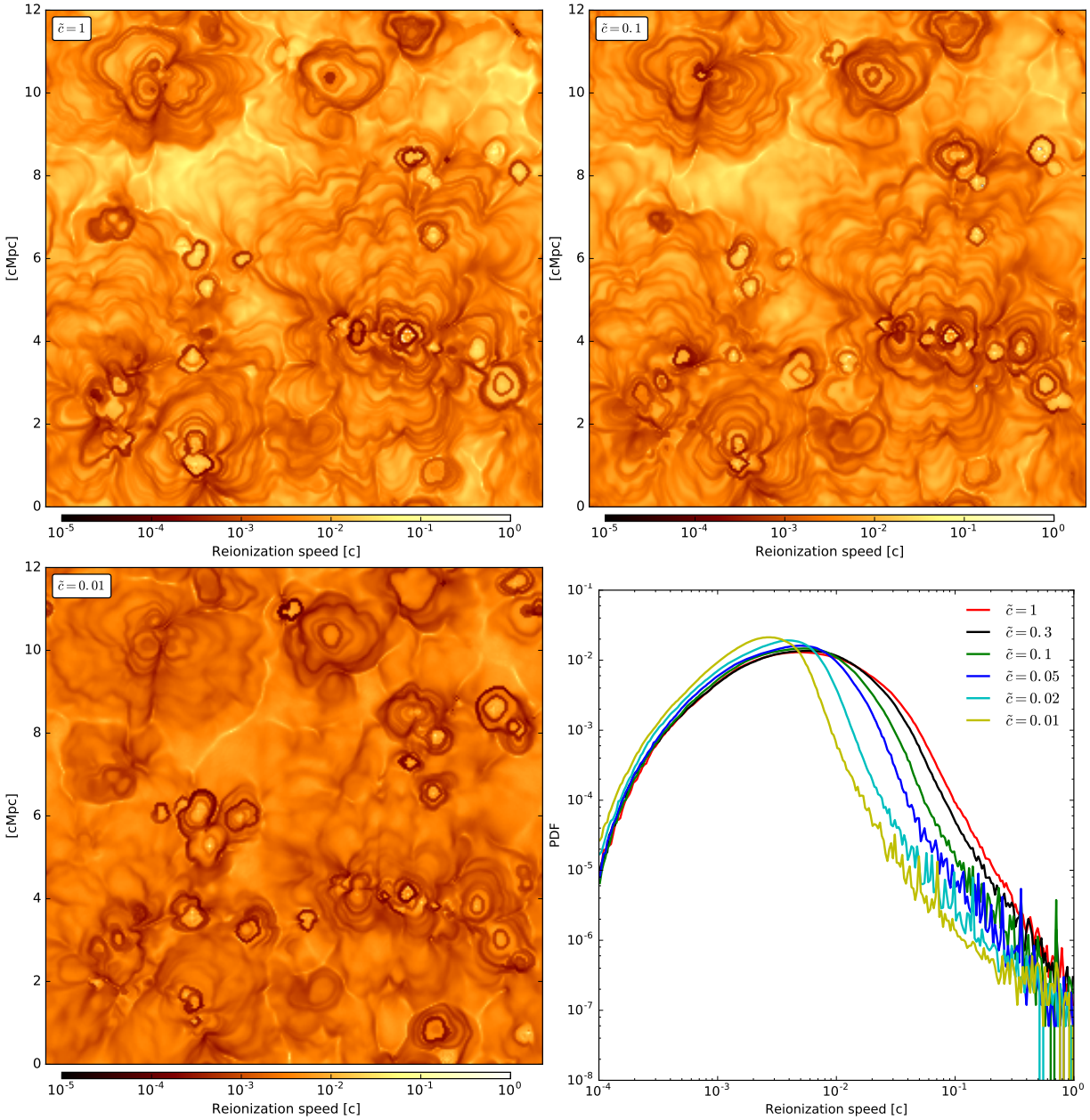

Figure 4. Maps and PDF of reionization front speeds for runs with different reduced speeds of light. Front speeds are expressed in units of the real speed of light.

- In over-dense regions, where adjacent cells have simultaneous star forming events.
- In under-dense regions, during the merging of two ionization fronts.

These spurious speeds represents a small fraction of the volume (with a fraction of $8 \cdot 10^{-5}$ in the worst case).On the PDF, we observe that limited light speeds do not avoid the presence of fronts speeds over its value. For instance, there are still front speeds of 10^{-1} when $\tilde{c} = 10^{-2}$ but the probability to find such a speed in the volume is significantly reduced. We found an average and most probable front speed going from respectively $\approx$ 2400km.s^{-1} and $\approx$ 1400km.s^{-1} for the $\tilde{c} = 1$ run to $\approx$ 1000km.s^{-1} and $\approx$ 800km.s^{-1} for the $\tilde{c} = 0.01$ run. It should be noted that this statistic is taken on the full reionization history.

In the maps, the concentric 'rings' with large and small speeds fronts is induced by the consecutive events of star formation. Reionization fronts can only expand if there are internal radiative sources, but star formation is not continuous and happens in a bursty manner. So fronts stop their progress during the time between two consecutive star formation events. The number of these concentric pattern decrease with the speed of light, With the $\tilde{c} = 0.01$ run the map is lot smoother than the $\tilde{c} = 1$ run.

3.5 Speed of ionization fronts as a function of redshift

We show in the last section that reducing the speed of light in the simulation limit the probability to find a front speed above this limit. In the two previous section we have associated a redshift and a speed at each point of space. In this section we analyse the evolution of the reionization front speed as a function of redshift. Fig. 5 presents the distributions of fronts speed as a function of redshift, as well as the evolution of the average fronts speed for different RSLA.

We first focus on the 2D histograms that show the redshift evolution of the front speeds distribution. In the $\tilde{c} = 1$ run, we observe that for z>8, the distributions of speeds are always between $\approx 10^{-1}$ and $\approx 10^{-4}$. This phase is then followed by a quick acceleration peak or plume. We observe a two stages process : first light escapes over-dense regions at an average constant speed and second, the percolation of ionized bubbles allows the light to reach under-dense regions. In these regions, the fronts speeds are not limited by the interaction with baryons. The light is free to fill the voids and fronts speeds are able to reach the real speed of light. After the reionization, when ionization bubbles have collapsed, the probability to find an high speed front drops suddenly, as the whole volume is ionized.

In the $\tilde{c} = 0.1$ run, the first phase is not impacted by the RSLA: even with $\tilde{c} = 1$ the front speeds where already lower than $\approx 10^{-1}$. The main difference appears in the second phase: the $z < 8$ peak is reduced by the RSLA. With $\tilde{c} = 1$ the fronts are able to reach speeds greater than 0.1c, by setting $\tilde{c} = 0.1$ velocities of this fronts are limited to $\approx 0.1c$ in an artificial manner : the end of the reionization is slightly delayed.

In the $\tilde{c} = 0.01$ run, the propagation of light is already limited at the beginning of the reionization. In the two previous runs, fronts speeds where already greater than $\approx 0.01c$ since the beginning of the reionization. This leads to an important cumulative delay in the reionization redshift. Moreover, the final peak is almost totally smoothed.

Looking now at the average fronts speeds as a function of redshift, we clearly measure an almost constant value followed by an acceleration for redshift $z < 8$. In the $z > 8$ constant phase, the average front speed goes from $4.1 \cdot 10^{-3}[c]$ for the $\tilde{c} = 1$ run to $2.2 \cdot 10^{-3}[c]$ for the $\tilde{c} = 0.01$ run. This constant phase is the same that we observe on Fig. 2, the ionization rate is constant when the fronts speed are constants. In the constant phase, all runs with RSLA higher than 0.05 have a similar average speed and ionization rate. But for RSLA lower than 0.05 both are limited from the beginning of the reionization. This link between ionization rate and front speed is also visible on Fig. 3 : the PDF of reionization redshift remains the same for redshift $z > 8$ if $\tilde{c} > 0.05$, but presents a shift starting at redshift $z \approx 14$ for $\tilde{c} < 0.05$. Meanwhile, the second-stage acceleration for redshifts $z < 8$ is significantly impacted by the RSLA. With a large speed of light the box flashes faster at the end of the reionization than with lower values. This final acceleration correspond to the light reaching under dense regions and in all cases the average front speed is limited by the RSLA, even though $\tilde{c} = 0.3$ is quite consistent with $\tilde{c} = 1$. To sum up reduced speed of lights $\tilde{c} > 0.05$ present the proper behaviour for the first stage of the propagation of fronts but will likely present a delay for the overlap if $\tilde{c} < 0.3$.

4 CONCLUSIONS

We presented a method to compute ionization fronts speeds a posteriori using reionization maps. With this method we found that reducing the speed of light in our simulations tends to impact the fronts and their propagation.

Analysing the average fronts speeds as a function of redshift, we observe that the reionization happens in two stages. First a constant speed phase, followed by a acceleration phase. During the constant speed phase, the average value do not depends of $\tilde{c}$ for $\tilde{c} > 0.05$. In all case, the acceleration phase is impacted by the choice of the RSLA, but reasonable convergence can be achieved for $\tilde{c} > 0.1-0.3$. Observations from e.g. Fan et al. (2006) impose time constraints for the very end of the reionization. But we show that the RSLA can significantly impact the speed of the reionization especially toward the overlap. Its seems then difficult to strictly conciliate RSLAs with a well timed reionization by observational constraints.

In conclusion, the RSLA can be a good approximation down to $\tilde{c} = 0.05$, if the goal is to analyse dense regions behaviour. Things are more complicated while considering the ionization of cosmic voids, as in those ones the fronts speeds can be as large as c, the RSLA is always a limiting factor.

ACKNOWLEDGEMENTS

This work is supported by the ANR ORAGE grant ANR-14-CE33-0016 of the French Agence Nationale de la Recherche.

REFERENCES

Aubert D., Teyssier R., 2008, Monthly Notices of the Royal Astronomical Society, 387, 295
Aubert D., Deparis N., Ocvirk P., 2015, Monthly Notices of the Royal Astronomical Society, 454, 1012
Bouwens R. J., et al., 2015, The Astrophysical Journal, 803, 34
Fan X., Carilli C. L., Keating B., 2006, Annual Review of Astronomy and Astrophysics, 44, 415
Gnedin N. Y., 2014, arXiv:1403.4245 [astro-ph]
Gnedin N. Y., Abel T., 2001a, New Astron., 6, 437
Gnedin N. Y., Abel T., 2001b, New Astronomy, 6, 437
González M., Audit E., Huynh P., 2007, A&A, 464, 429
Levermore C. D., 1984, J. Quant. Spectrosc. Radiative Transfer, 31, 149
Maselli A., Ferrara A., Ciardi B., 2003, MNRAS, 345, 379
Mellema G., Iliev I. T., Alvarez M. A., Shapiro P. R., 2006, New Astron., 11, 374
Ocvirk P., et al., 2015, preprint, 1511, 11
Semelin B., Combes F., Baek S., 2007, A&A, 474, 365

This paper has been typeset from a TEX/LATEX file prepared by the author.

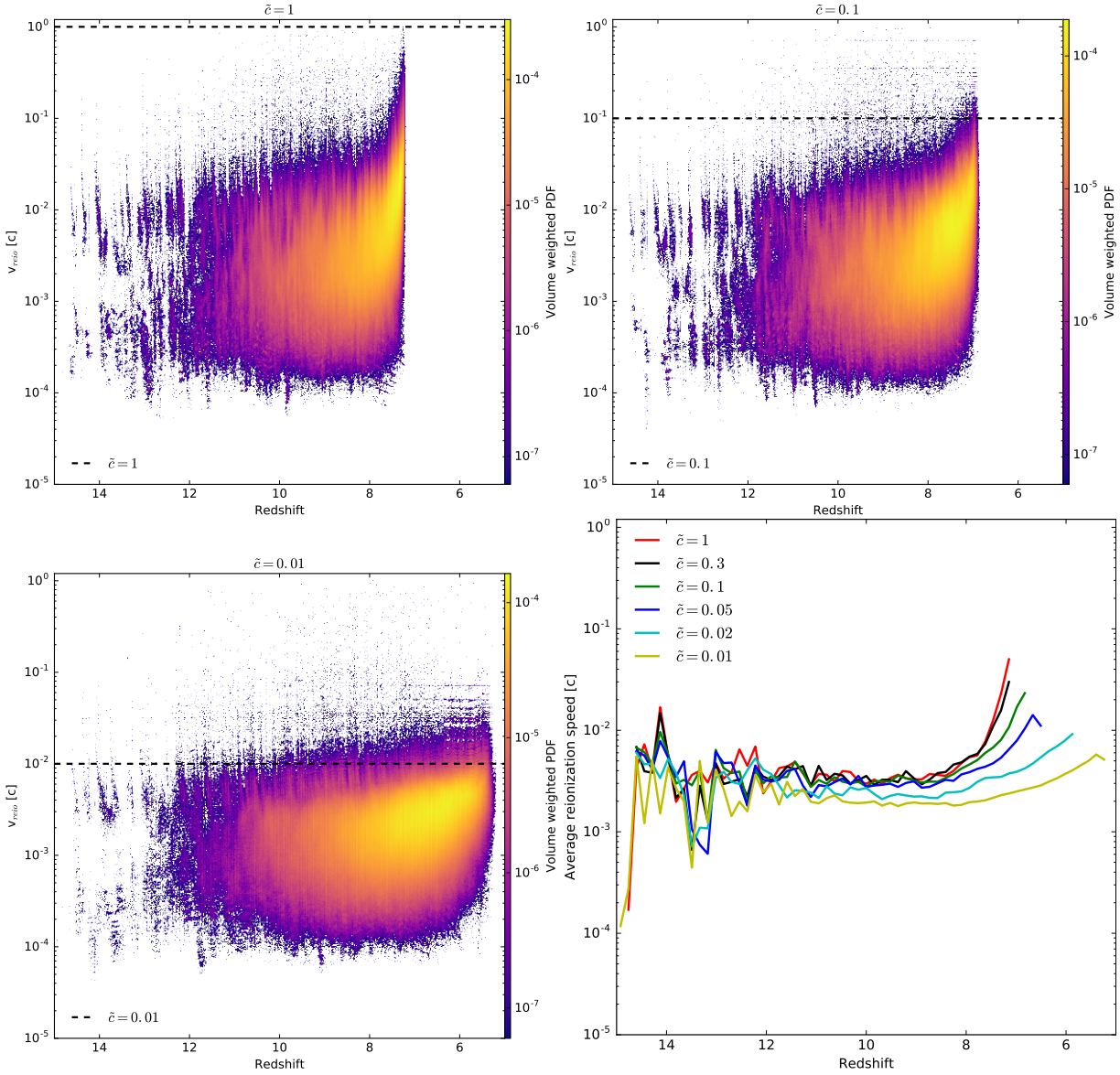

Figure 5. 2D histograms and average of reionization speeds in units of the real speed of light as a function of redshift for different RSLA. The horizontal dashed line represents $\tilde{c}$ the reduced light speed used in the simulation.